MEASUREMENTS ON SEXTUPOLE AND OCTUPOLE LENSES.

1. General data.

In the synchrotron 20 sextupoles and 20 octupoles are used. One sextupole and one octupole, mounted together on a support, are shown in fig. 1. The characteristics are as follows:

	Sextupoles	Octupoles	Kicker windings on octupoles	
distance pole tips to axis	68.5 mm	69.5 mm		
radius of curvature pole tips	36 mm	12.5 mm		
physical length of poles	270 mm	390 mm		
number of turns per coil	72	34	90	135
number of coils	3	8	2	2
cross-section of turns without insulation	6.5x2.8 mm	6.5x2.8 mm	3.3x1.5 mm	
with "	6.8x3.2 mm	6.8x3.2 mm	3.58x1.8 mm	
resistance per lens (16°C)	161 mΩ	251 mΩ	2.2 Ω	
inductance per lens (at 2A, 50 c/s)	15.4 mH	24.2 mH	~200 mH	
thickness of steel laminations	0.35 mm	0.35 mm		
laminations glued together with bakelite varnish				
coercive force of steel	0.25oersted	0.25oersted		
max. excitation current	100 A	100 A	22 A	
max. r.m.s. exc. current	21 A	32 A	7 A	

2. Sextupole measurements.

a) Dynamic gradient vs. current.

A lens was excited with current pulses of the shape shown in fig. 2. The gradient was measured as a function of current with 600 mm long measuring coils parallel to the axis. In this way the gradient integrated over the total length was measured, stray fields at the ends included. The measurement was done at r = 3 cm. Fig. 3 shows the result. No saturation can be seen at high currents. In fact it can be calculated that the induction in the steel does not exceed 5000 gauss at peak current, except in the sharp corners of the poles.

b) Dynamic gradient vs. radius.

At currents of 50 A and 100 A a relative measurement was made of the gradient as a function of r at intervals of 1 cm between r = -6 and r = + 6 cm. The long coils mentioned above were used again. The result is shown in fig. 4. No difference between 50 A and 100 A was found.

c) Remanent field vs. r.

After exciting the lens many times with the pulse shape of fig. 2, the remanent field, integrated over the total length of the lens in including the stray field, was measured as a function of r (fig. 5). The asymmetry is probably caused by different coercive force of the different poles, despite the mixing of laminations during manufacture. In any case, the remanent field seems to be small enough to make demagnetizing between acceleration cycles unnecessary.

d) Comparison between lenses.

The dynamic gradient at a current of 100 A and r = 3 was measured in all lenses by comparison to a reference lens. It was found that the r.m.s. fluctuation is 0.6 o/o.
The remanent field at r = 6 was also measured in all lenses. The average value found was 0.255 gauss. m (integrated over the length), with a r.m.s. fluctuation of 0.027 gauss.m.

3. Octupole measurements.

a) Dynamic gradient vs. current.

The integrated gradient was measured at r = 4 cm and r = 6 cm (fig. 6) A slight curvature due to saturation can be detected at high currents.

b) Dynamic gradient vs. radius.

This was measured at 50 A and at 100 A excitation current. No difference was found (fig. 7).

d) Kicker field vs. current.

The kicker coils were excited with a pulse, similar in shape to that of fig. 2. In fig. 8 the integrated field-strength at r = 0 and r = 6 cm is shown as a function of current. No saturation effects are noticeable.

e) Kicker field vs. radius.

This was measured at i = 20 A in the median plane and at z = 1.5 cm. In fig. 10 the relative deviation, compared with the value on the orbit, is shown.

f) Remanent field vs. radius.

After exciting both octupole and kicker windings many times, the remanent field was measured. As seen from fig. 9, the value is not very high. Probably no demagnetization between cycles is necessary.

g) Comparison between lenses (octupole).

The dynamic gradient at a current of 100 A and r = 4 was measured in all lenses by comparison with a reference. A r.m.s. fluctuation of 0.34 o/o was found.
The remanent field at r = 6 was also measured. The average value of 0.55 gauss.m was found, with a r.m.s. fluctuation of 8 o/o.

h) Comparison between lenses (kicker).

The field on the orbit at a current of 20 A was measured in all lenses, compared to a reference. The r.m.s. fluctuation was found to be 0.15 o/o. It is not necessary that the kickers are exactly equal, as they will be used separately. The comparison was made as a check on irregularities in the manufacturing process.

S.van der Meer

/fv

Distribution: Magnet Group
Parameter Committee

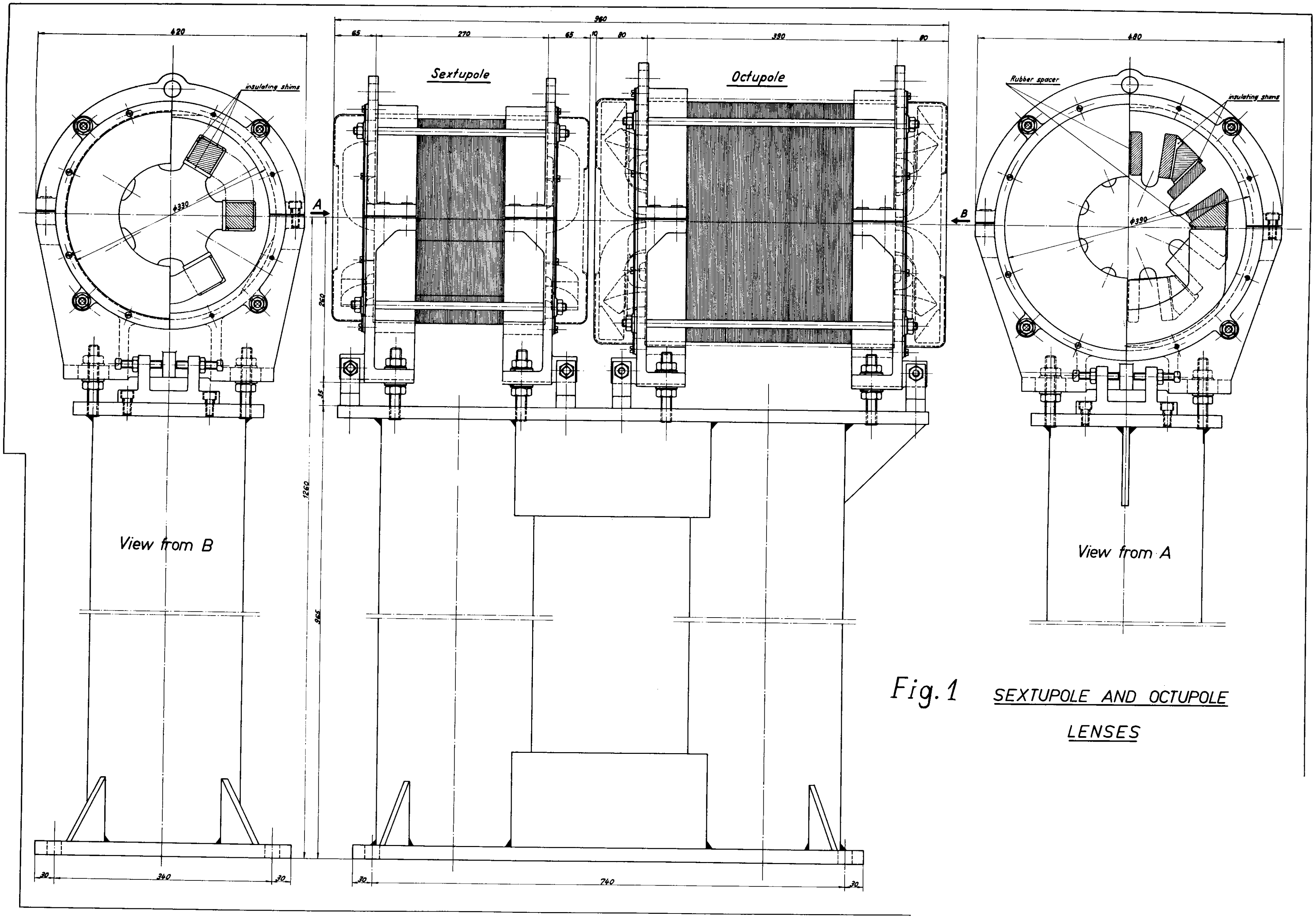

Fig. 1 SEXTUPOLE AND OCTUPOLE LENSES

SIS. R59/539

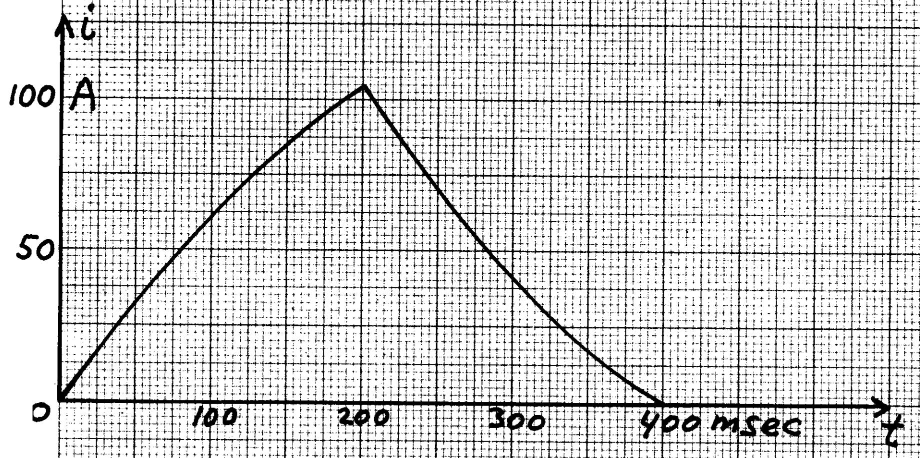
i
100 A
50
0
100
200
300
400 msec
t

Fig. 2

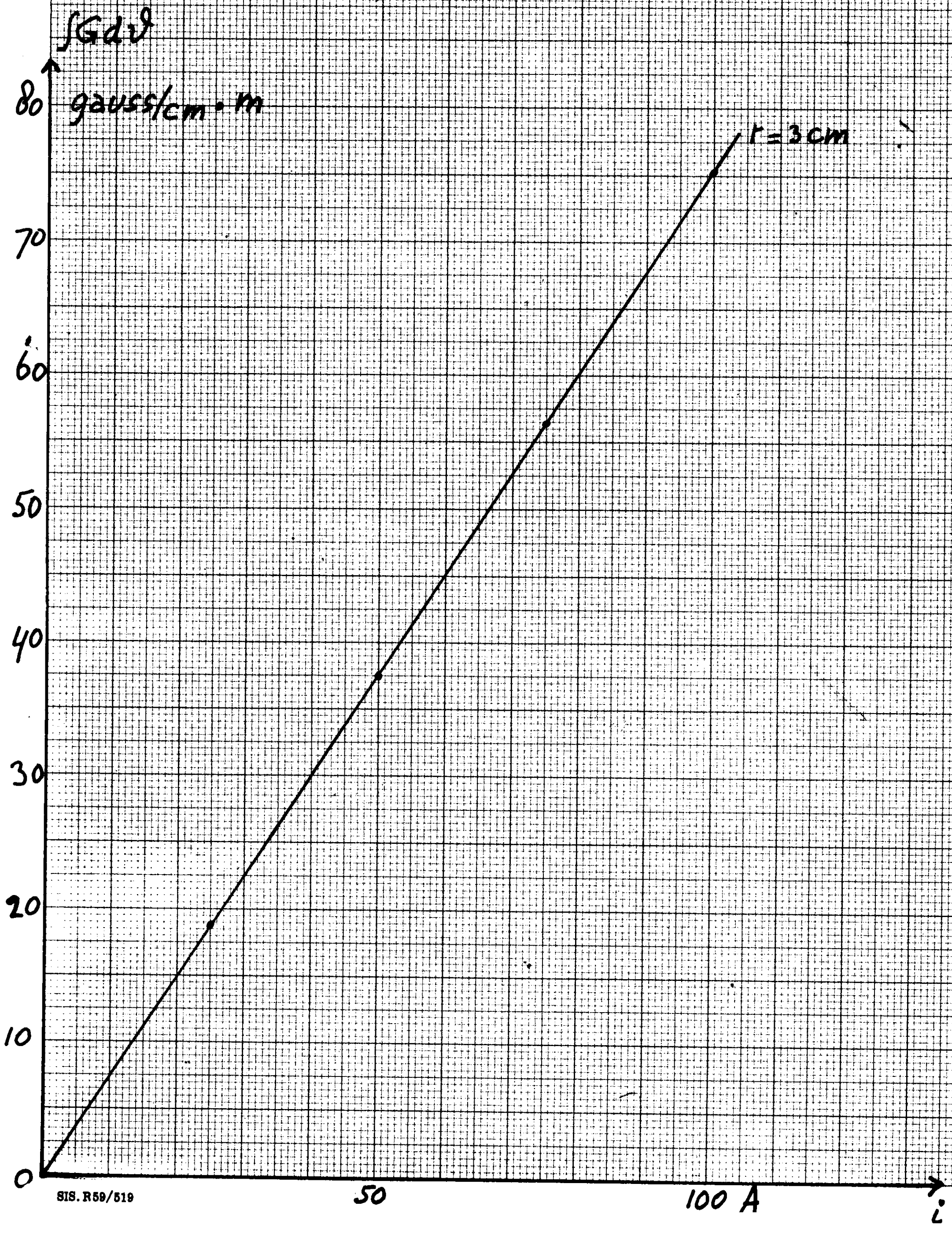
∫Gdϑ
gauss/cm · m
80
70
60
50
40
30
20
10
0
r = 3 cm
50
100 A
i

Fig. 3

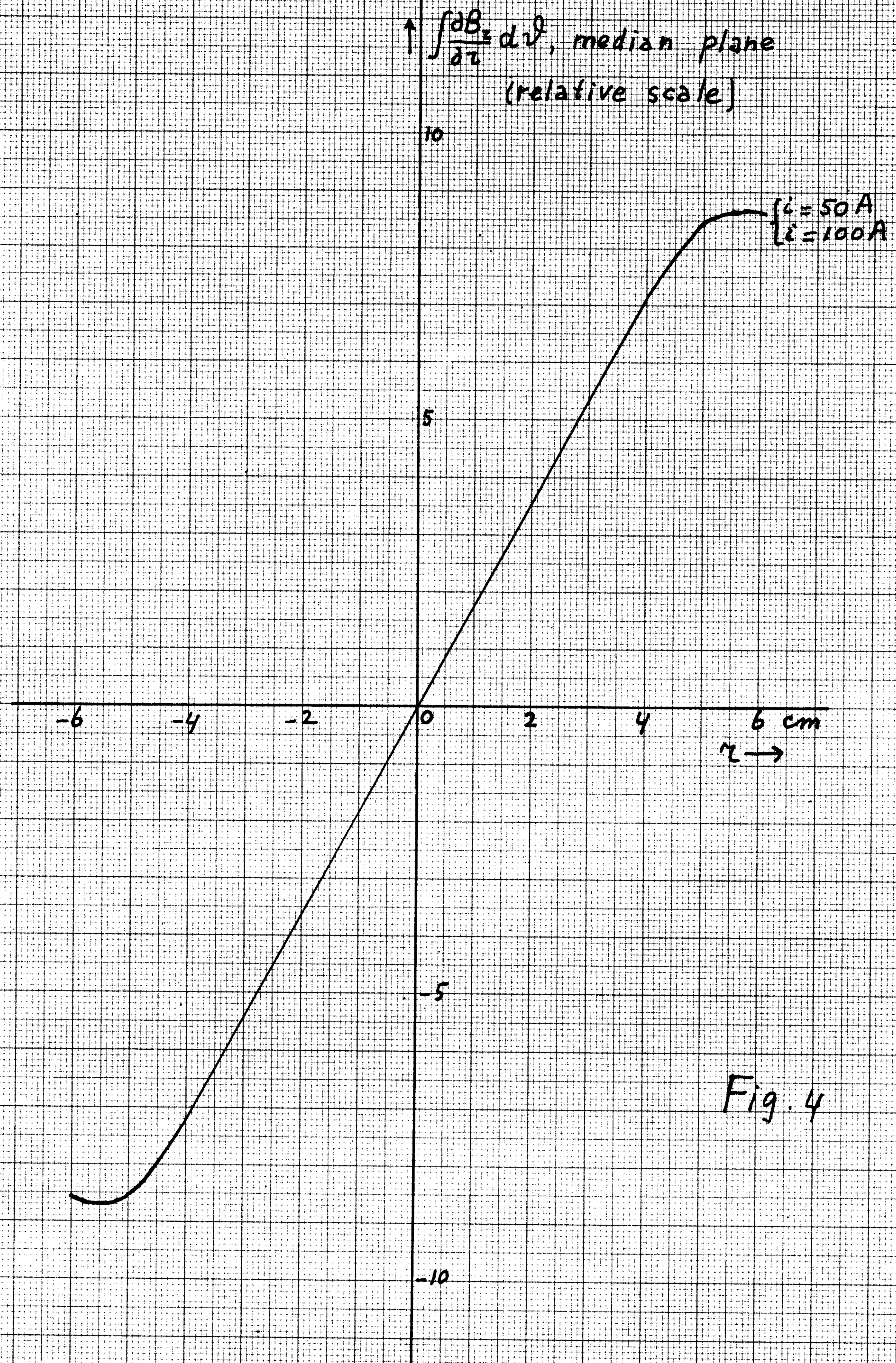

$\int \frac{\partial B_z}{\partial r} d\vartheta$, median plane
(relative scale)
10
5
-5
-10
-6
-4
-2
0
2
4
6 cm
r →
i = 50 A
i = 100 A

Fig. 4

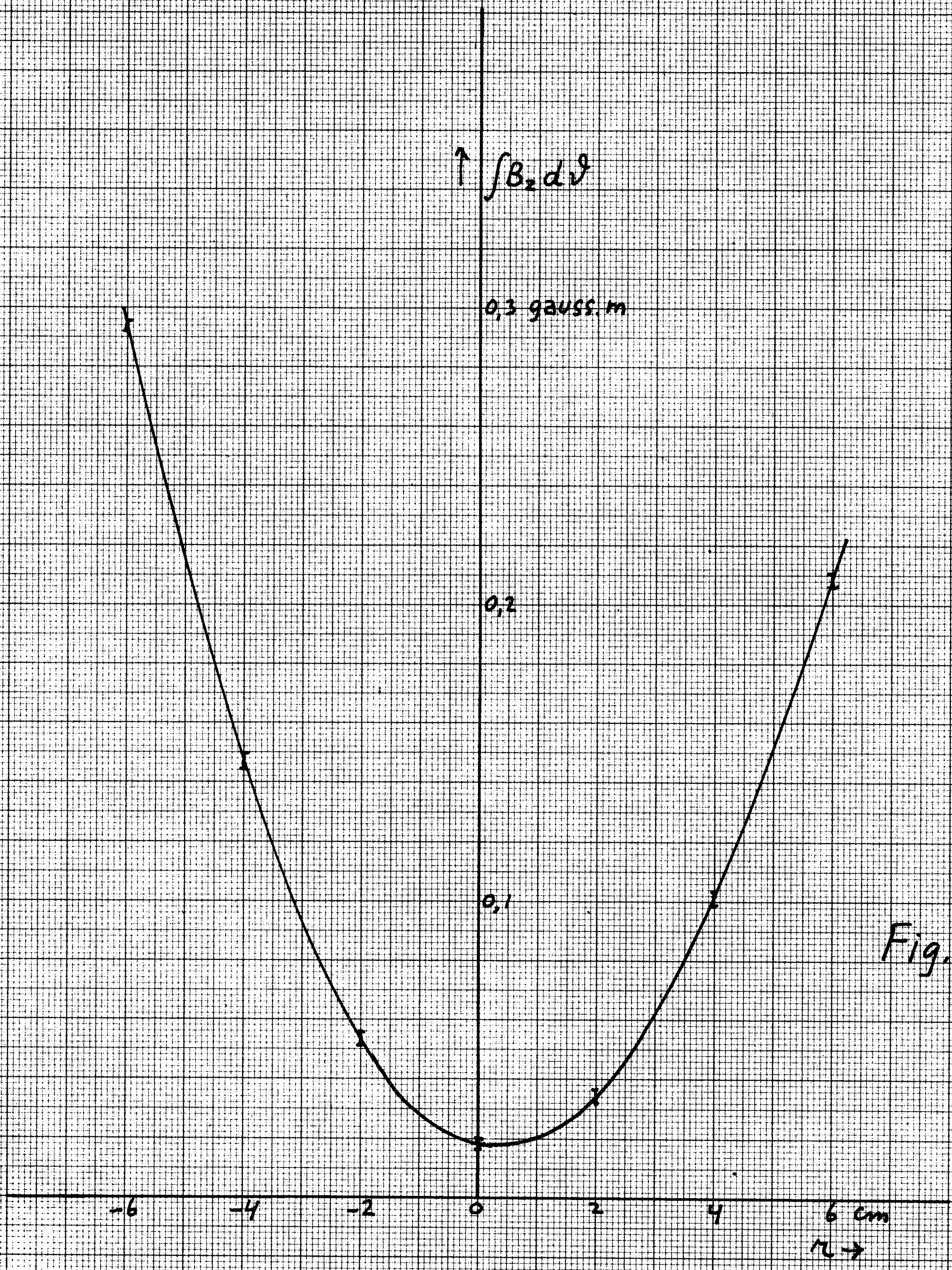

Fig. 5

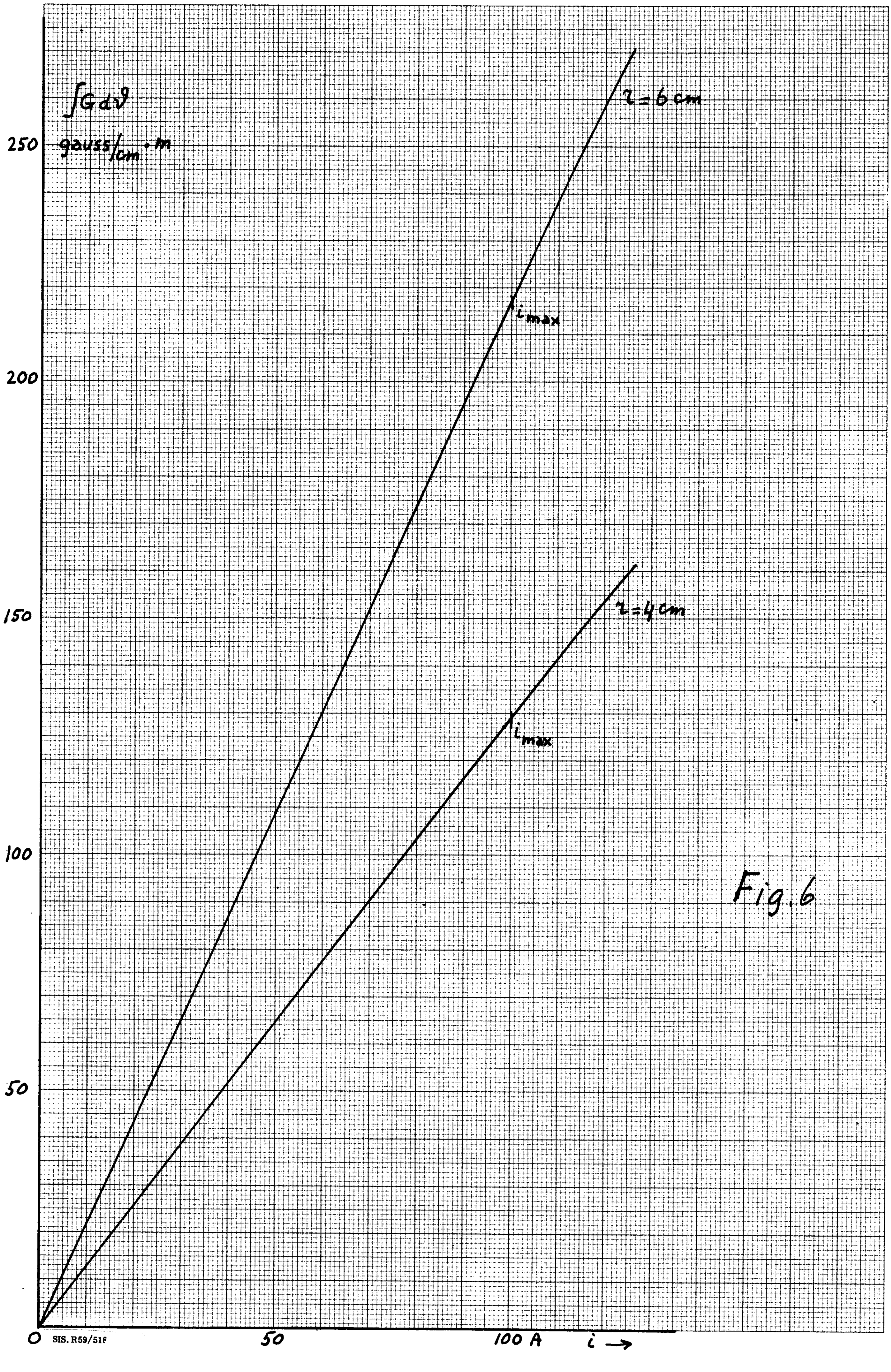
∫G dϑ
gauss/cm · m
250
200
150
100
50
0
50
100 A
i →
r = 6 cm
r = 4 cm
i max
i max
SIS. R59/518

Fig.6

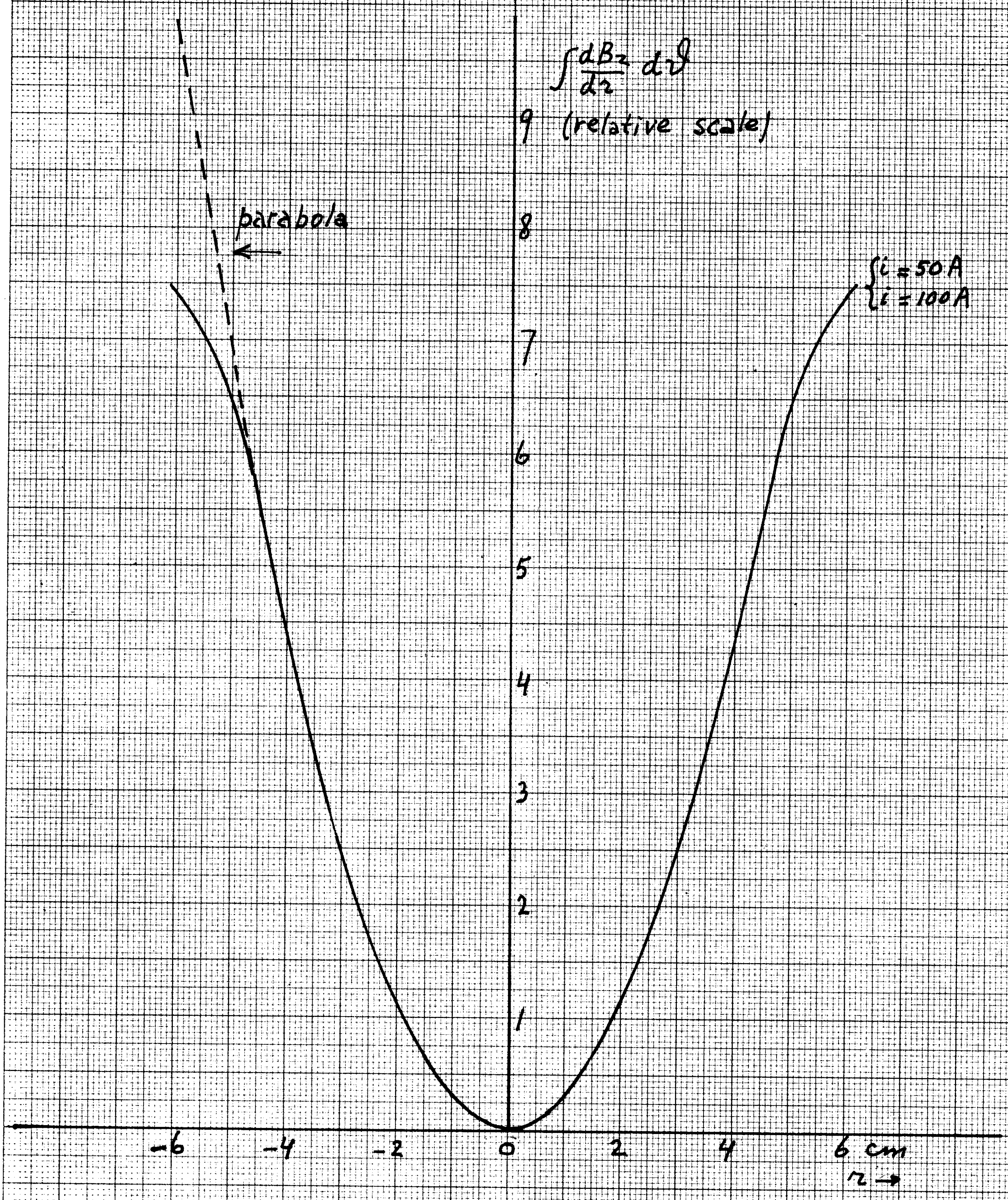
$\int \frac{dB_z}{dr} d\vartheta$
(relative scale)
parabola
$i = 50A$
$i = 100A$
9
8
7
6
5
4
3
2
1
-6
-4
-2
0
2
4
6 cm
r →

Fig. 7

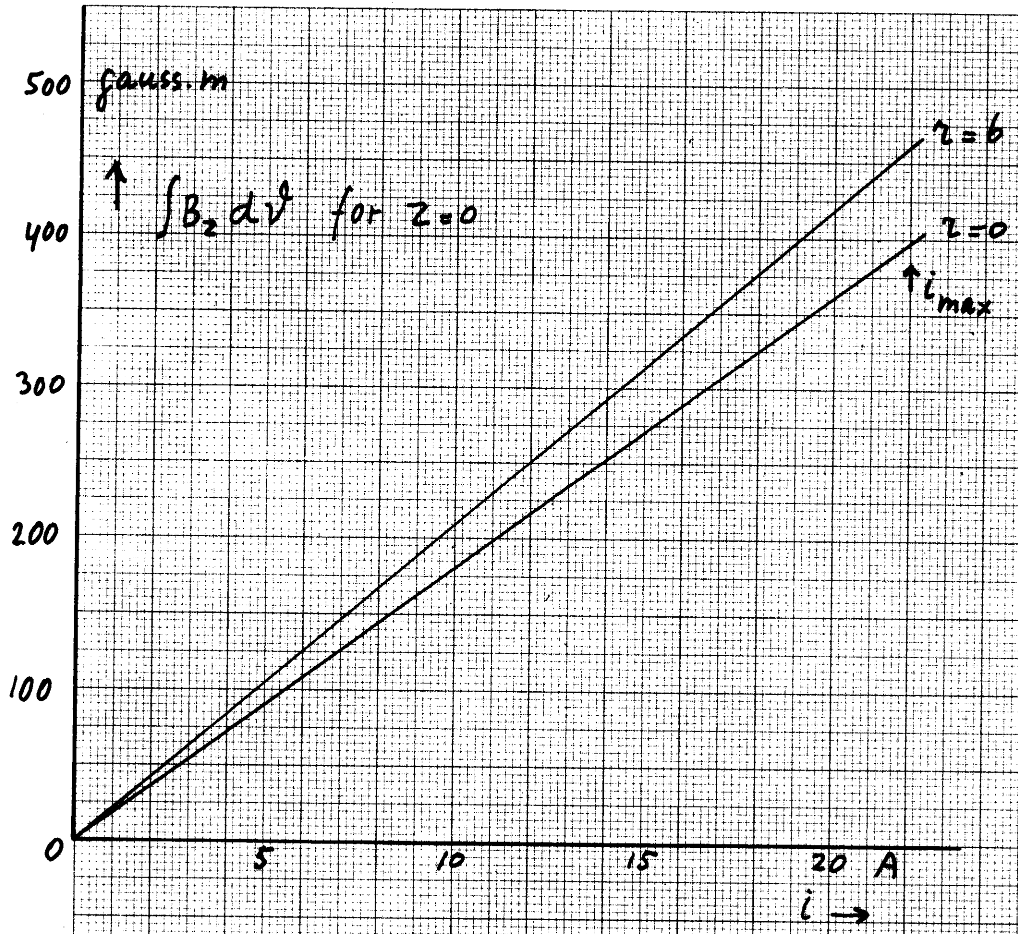

500 gauss. m
400
300
200
100
0
$\uparrow \int B_z \, d\vartheta$ for $z = 0$
$z = 6$
$z = 0$
$\uparrow i_{max}$
5
10
15
20
A
$i \rightarrow$

Fig.8

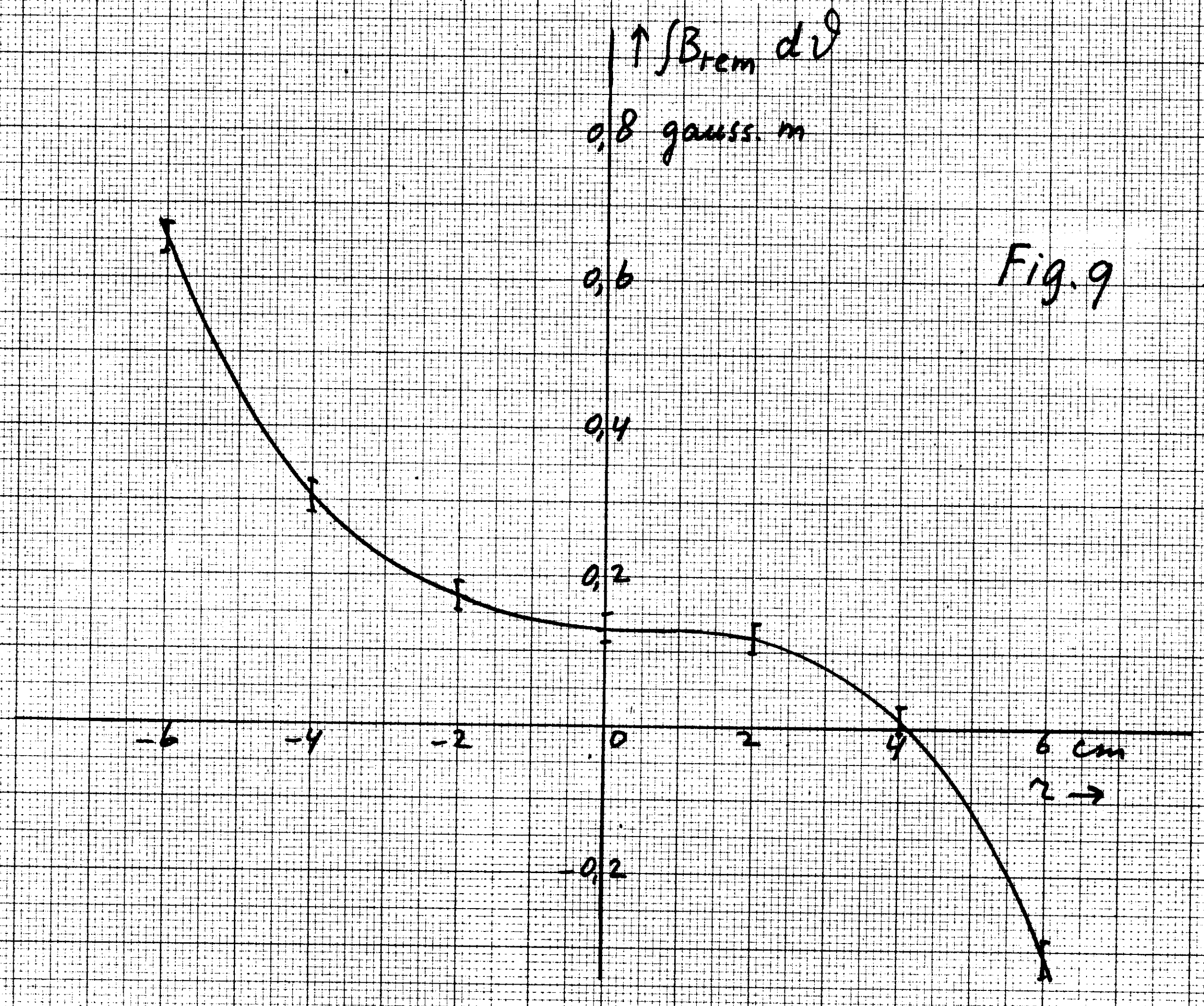

$\uparrow \int B_{rem} \, d\vartheta$
0,8 gauss. m
0,6
0,4
0,2
-0,2
-6
-4
-2
0
2
4
6 cm
$z \rightarrow$

Fig.9

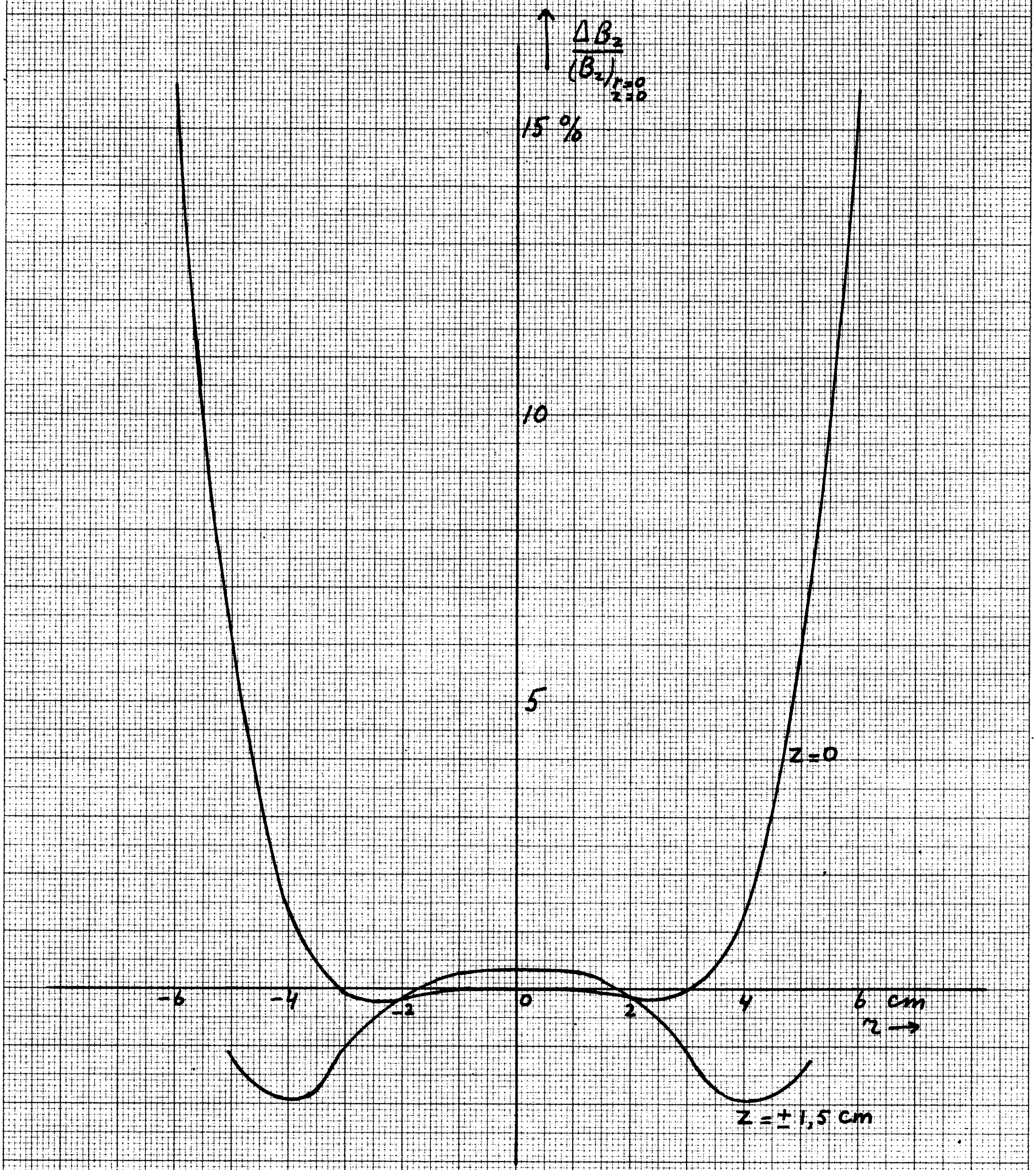

Fig. 10